CHAPTER 3

Modeling of Doubly Fed Induction Generation (DFIG) Converter Controls

In this chapter, the major effort is devoted to converter controls of DFIG. Differences between drive control and grid integration control are discussed before any presentation of controls. To refresh our memory on drive control, rotor flux-oriented control for an induction machine is first presented, followed by DFIG's rotor-side converter (RSC) control and grid-side converter (GSC) control. With a converter being considered as a controllable AC voltage source with a controllable frequency, magnitude, and phase angle, the entire DFIG system model (with converter controls) can now be built in the *dq*-reference frame.

Modeling and Analysis of Doubly Fed Induction Generator Wind Energy Systems.
http://dx.doi.org/10.1016/B978-0-12-802969-5.00003-2

This chapter presents two simulation examples. The first one is a simulation example in PSCAD with power electronic switching details. The purpose of the demonstration is to show that converter voltage outputs after filters are sinusoidal. Readers can then build visual connections between control of *abc* sinusoidal waveforms versus vector control or control of *dq* variables. The second one is a demonstration of DFIG converter control using the overall DFIG dynamic model.

3.1 ROTOR FLUX-ORIENTED INDUCTION MACHINE CONTROL

Before discussing DFIG converter control, let us review a few concepts related to an induction machine control. Interested readers can refer AC drive textbooks such as [1], for a variety of drive controls, including rotor flux-oriented control and stator flux-oriented control.

From a control engineer's perspective, the first thing to notice is the input/output of the plant: what will be adjusted and which measurements will be used as signals. In the case of induction machine control, we would like to adjust the stator voltage to realize speed control. Therefore, stator voltage is the input of the plant while speed is the output. The stator voltage can be generated by a DC/AC voltage source converter. Through adjusting pulse width modulation (PMW)'s control signals, the output voltage can have a controllable magnitude, frequency, and angle. Note that the output voltage directly from the converter is of discrete voltage levels. It can be decomposed into a fundamental frequency component and higher-order harmonic components with the frequencies at the order of the switching frequency. For an IGBT voltage source converter, the switching frequency is more than ten times of the fundamental frequency. For example, for a 50-Hz system, the switching frequency could be 750 Hz.

Averaging is a modeling and analysis technique popularly applied in power electronics [2]. With switches, converters generate voltages with discrete levels. Through averaging the converter output voltage over a switching period, the higher-order harmonics will all be gone. Only the lower-order harmonics will be considered in modeling. Averaging technique greatly simplifies modeling. It is also reasonable to ignore higher-order harmonics since an inductive filter after the converter or the inductance in windings can get rid of those harmonics. Another benefit of average models is that discrete switching is now ignored from modeling. Average models are continuous dynamic models.

For the analytical models built throughout the textbook, the underlying assumption is that the models are average models. Ultimately, the converter control is expected to generate the stator voltage reference signals. These sinusoidal signals will be fed into the PWM of a VSC to generate pulses to six gates for a typical two-level voltage source converter.

Details of PWM and IGBT switching will not be discussed in this book as these can be found in a typical power electronics textbook. Converters are sensitive to over currents. Therefore, currents through a converter are expected to be regulated very quickly and follow their references. For an induction machine, a constant flux is desired. In summary, an induction machine control should include speed (torque) control, flux control, and current control. In addition, the current control should be much faster than the torque and flux control. Therefore, when designing current control, we can treat the flux and torque as constant, while when we design the torque or flux control, we can assume that the currents can follow their commands immediately. The current control design and the torque/flux control design can be done separately with these assumptions.

3.1.1 Torque/Flux Control

The principal of the decoupled torque/flux control is explained in the following paragraphs. From Chapter 2, we know that the torque can be expressed in terms of air gap flux linkage and the stator current.

$$T_{\mathrm{e}} = \frac{3}{2}\frac{P}{2}\mathcal{R}\left(j\overline{\psi_{\mathrm{m}}}\overline{I_{\mathrm{s}}}^{*}\right) \tag{3.1}$$

Note that the air gap flux linkage and the rotor flux linkage can be related as follows:

$$\overline{\psi_{\mathrm{r}}} = L_{\mathrm{r}}\overline{I_{\mathrm{r}}} + L_{\mathrm{m}}\overline{I_{\mathrm{s}}} \tag{3.2}$$

$$= L_{\mathrm{r}}(\overline{I_{\mathrm{r}}} + \overline{I_{\mathrm{s}}}) - L_{\mathrm{lr}}\overline{I_{\mathrm{s}}} \tag{3.3}$$

$$= \frac{L_{\mathrm{r}}}{L_{\mathrm{m}}}\overline{\psi_{\mathrm{m}}} - L_{\mathrm{lr}}\overline{I_{\mathrm{s}}} \tag{3.4}$$

Therefore, the torque can be expressed in terms of the rotor flux linkage and the stator current.

$$T_{\mathrm{e}} = \frac{3}{2}\frac{P}{2}\mathcal{R}\left(j\frac{L_{\mathrm{m}}}{L_r}\left(\overline{\psi_{\mathrm{r}}} + L_{\mathrm{lr}}\overline{I_{\mathrm{s}}}\right)\overline{I_{\mathrm{s}}}^{*}\right) \tag{3.5}$$

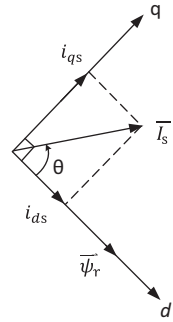

Figure 3.1 Current complex vector decomposed based on the rotor flux-oriented reference frame.

$$= \frac{3}{2}\frac{P}{2}\frac{L_m}{L_r}\mathcal{R}\left(j\overline{\psi_r I_s}^*\right) \tag{3.6}$$

$$= \frac{3}{2}\frac{P}{2}\frac{L_m}{L_r}\left(\psi_{dr} i_{qs} - \psi_{qr} i_{ds}\right) \tag{3.7}$$

It is easily seen in Fig. 3.1 that when the d-axis is aligned with the rotor flux $\overrightarrow{\psi_r}$ ($\overline{\psi_r}$ can be decoupled as $\psi_{dr} = \hat{\psi}_r$ and $\psi_{qr} = 0$), $\overline{I_s}$ can be decoupled as i_{qs} and i_{ds} and the electromagnetic torque T_e is only related to the q-axis stator current i_{qs}.

$$T_e = k\hat{\psi}_r i_{qs} \tag{3.8}$$

where $k = \frac{3}{2}\frac{P}{2}\frac{L_m}{Lr}$. If the rotor flux magnitude $\hat{\psi}_r$ is constant, then T_e and i_{qs} has a linear relationship. If we want to adjust the torque, we can adjust i_{qs} only. On the other hand, we also need to make sure that adjusting i_{qs} will not change the rotor flux magnitude. This can be proved by the following derivation.

The relationship between $\overline{\psi_r}$ and $\overline{I_s}$ is shown below:

$$\overline{\psi_r} = L_r\overline{i_r} + L_m\overline{i_s} \Rightarrow \overline{i_r} = \frac{1}{L_r}(\overline{\psi_r} - L_m\overline{i_s}) \tag{3.9}$$

The relationship between the rotor voltage and the rotor flux is shown as follows:

$$\overline{V_r} = 0 = R_r\overline{i_r} + \frac{d\overline{\psi_r}}{dt} + j\omega_{sl}\overline{\psi_r} \tag{3.10}$$

where ω_{sl} is the slip frequency.

Therefore, for qd-axis variables, we find the following relationship:

$$\begin{cases} 0 = \frac{R_\mathrm{r}}{L_\mathrm{r}}(\psi_{qr} - L_\mathrm{m} i_{qs}) + \frac{\mathrm{d}\psi_{qr}}{\mathrm{d}t} + \omega_{sl}\psi_{dr} \\ 0 = \frac{R_\mathrm{r}}{L_\mathrm{r}}(\psi_{dr} - L_\mathrm{m} i_{ds}) + \frac{\mathrm{d}\psi_{\mathrm{d}r}}{\mathrm{d}t} - \omega_{sl}\psi_{qr} \end{cases} \tag{3.11}$$

Since $\psi_{qr} = 0$, its derivative $\frac{\mathrm{d}\psi_{qr}}{\mathrm{d}t}$ also equals zero. In addition, at steady state, the flux is kept constant. Therefore $\frac{\mathrm{d}\psi_{\mathrm{d}r}}{\mathrm{d}t} = 0$. Thus, we have

$$\omega_{sl} = \frac{R \cdot L_\mathrm{m}}{L_\mathrm{r} \cdot \hat{\psi}_\mathrm{r}} i_{qs} \tag{3.12}$$

$$\psi_{dr} = L_\mathrm{m} i_{ds} \tag{3.13}$$

The rotor flux is related to the d-axis stator current only. Therefore, changing i_{qs} will not impact the steady-state rotor flux magnitude. The aforementioned analysis demonstrates that the torque and flux can be controlled in a decoupled fashion. Given a constant rotor flux, torque is proportional to the q-axis stator current. To track a torque or flux reference, proportional integral controllers are employed to generate the qd-axis current commands. These commands will be tracked by the current controllers.

3.1.2 Inner Current Control

To derive a current control strategy, first of all, we need to find the plant model where the outputs of the plant are current signals and the inputs of the plant model are converter voltages. The control will be based on the rotor flux-oriented reference frame. Therefore, the plant model is also based on the rotor flux-oriented reference frame.

Let us review the relationship between flux linkages and currents.

$$\psi_{qr} = L_\mathrm{r} i_{qr} + L_\mathrm{m} i_{qs} \tag{3.14}$$

$$\psi_{dr} = L_\mathrm{r} i_{dr} + L_\mathrm{m} i_{ds} \tag{3.15}$$

Based on the condition of the rotor flux-oriented reference frame, we know that $\psi_{dr} = \hat{\psi}_r$ and $\psi_{qr} = 0$. Therefore, we have the following relationship between the stator current and the rotor current.

$$i_{qr} = -\frac{L_\mathrm{m}}{L_\mathrm{r}} i_{qs} \tag{3.16}$$

$$i_{dr} = -\frac{L_\mathrm{m}}{L_\mathrm{r}} \left(\hat{\psi}_\mathrm{r} - L_\mathrm{m} i_{ds} \right) \tag{3.17}$$

The stator flux linkages in the rotor flux-oriented reference frame can now be expressed by the stator currents and the rotor flux magnitude solely.

$$\psi_{qs} = \left(L_{\mathrm{s}} - \frac{L_{\mathrm{m}}^2}{L_{\mathrm{r}}}\right) i_{qs} = \sigma L_{\mathrm{s}} i_{qs} \tag{3.18}$$

$$\psi_{ds} = \left(L_{\mathrm{s}} - \frac{L_{\mathrm{m}}^2}{L_{\mathrm{r}}}\right) i_{ds} + \frac{L_{\mathrm{m}}}{L_{\mathrm{r}}}\hat{\psi}_{\mathrm{r}} = \sigma L_{\mathrm{s}} i_{ds} + \frac{L_{\mathrm{m}}}{L_{\mathrm{r}}}\hat{\psi}_{\mathrm{r}} \tag{3.19}$$

where $\sigma = 1 - \frac{L_{\mathrm{m}}^2}{L_{\mathrm{s}} L_{\mathrm{r}}}$.

In the rotor flux-oriented reference frame, the relationship of the stator voltage and the stator current can then be found as follows:

$$v_{qs} = r i_{qs} + \sigma L_{\mathrm{s}} \frac{\mathrm{d}i_{qs}}{\mathrm{d}t} + \sigma \omega L_{\mathrm{s}} i_{ds} + \omega \frac{L_{\mathrm{m}}}{L_{\mathrm{r}}}\hat{\psi}_{\mathrm{r}} \tag{3.20}$$

$$v_{ds} = r i_{ds} + \sigma L_{\mathrm{s}} \frac{\mathrm{d}i_{ds}}{\mathrm{d}t} - \sigma \omega L_{\mathrm{s}} i_{qs} \tag{3.21}$$

where ω is the rotor flux rotating speed. This speed should be the same as the electric frequency in the stator voltage and currents.

Feedforward techniques can be applied to design the current controllers for the *qd*-axis respectively. For simplicity, if we are not keen to have decoupled effect of *qd*-axis current tracking, we can also live with a feedback control without feedforward terms.

Define two variables

$$u_{qs} = v_{qs} - \sigma \omega L_{\mathrm{s}} i_{ds} - \omega \frac{L_{\mathrm{m}}}{L_{\mathrm{r}}}\hat{\psi}_{\mathrm{r}} \tag{3.22}$$

$$u_{ds} = v_{ds} + \sigma \omega L_{\mathrm{s}} i_{qs}. \tag{3.23}$$

Then, we can have two plant models:

$$\frac{i_{qs}}{u_{qs}} = \frac{1}{r + \sigma L_{\mathrm{s}} s} \tag{3.24}$$

$$\frac{i_{ds}}{u_{ds}} = \frac{1}{r + \sigma L_{\mathrm{s}} s} \tag{3.25}$$

We can design the feedback controller in the format of PI control to achieve desired bandwidth. Assume that the PI controller is $K_{\mathrm{P}} + K_i/s$. Then the open-loop transfer function (or loop gain) is

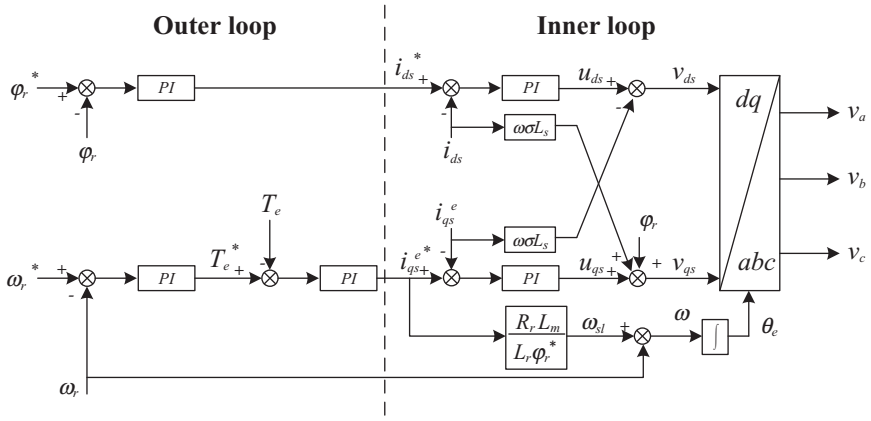

Figure 3.2 Induction machine control block diagram.

$$L(s) = \frac{K_{\mathrm{P}}(s + K_{\mathrm{P}}/K_i)}{s} \frac{1}{r + \sigma L_{\mathrm{s}} s}.$$

Let $K_i/K_{\mathrm{P}} = R/(\sigma L_{\mathrm{s}})$ so that the zero can cancel one of the poles. The loop gain now becomes:

$$L(s) = \frac{K_{\mathrm{P}}}{\sigma L_{\mathrm{s}} s}.$$

The closed-loop transfer function is

$$L_{\mathrm{cl}}(s) = \frac{1}{1 + \frac{\sigma L_{\mathrm{s}}}{K_{\mathrm{p}}} s}$$

If the desired bandwidth is ω_{B}, then $\omega_{\mathrm{B}} = \frac{K_{\mathrm{P}}}{\sigma L_{\mathrm{s}}}$. Based on this relationship, we can determine K_{P} and further determine K_i.

The overall control block diagram shown in Fig. 3.2 includes feedforward terms. The controller parameters can be obtained by trial and error or by analysis.

3.2 DFIG ROTOR SIDE CONVERTER CONTROL

The difference between a grid-integrated DFIG wind turbine and an induction machine resides in control objectives. For a DFIG, the converter

controls are to regulate real power (or torque) and reactive power (or voltage) send to the grid through RSC and GSC's output voltages. RSC's and GSC's AC-side output voltages are the inputs to the plants and the outputs from the converter controls.

DFIG converter controls have been well documented in the literature, *e.g.,* [3]. In this chapter, we will give a brief explanation of the vector control philosophy, the related plant models, and control design.

3.2.1 Outer Control

A RSC is connected to the rotor circuit. Therefore, the rotor currents should also be regulated to avoid overcurrent in the RSC. In that sense, we can reason that the inner current control for a RSC should be the rotor current control, while the outer control should be the real power (torque) and reactive power (ac voltage) control.

Unlike rotor flux-oriented control of an induction machine, DFIG's control relies on stator flux-oriented reference frame ($\psi_{qs} = 0$ or $v_{ds} = 0$). Since DFIG wind turbines are integrated to the grid and the grid voltage can be assumed as constant, the stator flux of the DFIG can be assumed as constant. In the literature, we may find other types of reference frames, e.g., grid flux (flux corresponding to the grid voltage) oriented reference frame, which is also reasonable.

We will express the torque by the stator flux and the rotor current to show that decoupling control is possible for a DFIG. Employing the same technique shown in the previous section, we find that

$$\overline{\psi}_{\mathrm{s}} = L_{\mathrm{s}}\bar{I}_{\mathrm{s}} + L_{\mathrm{m}}\bar{I}_{\mathrm{r}} \tag{3.26}$$

$$= \frac{L_{\mathrm{s}}}{L_{\mathrm{m}}}\overline{\psi}_{\mathrm{m}} - L_{\mathrm{ls}}\bar{I}_{\mathrm{r}} \tag{3.27}$$

Therefore, the torque expression can be found:

$$T_{\mathrm{e}} = \frac{3}{2}\frac{P}{2}\frac{L_{\mathrm{m}}}{L_{\mathrm{s}}}\left(\psi_{qs}i_{dr} - \psi_{ds}i_{qr}\right) \tag{3.28}$$

$$= -\frac{3}{2}\frac{P}{2}\frac{L_{\mathrm{m}}}{L_{\mathrm{s}}}\psi_{ds}i_{qr} \tag{3.29}$$

Note that in this book, we adopt the motor convention. Therefore, when we consider this is a generator, the output power is related to $-T_{\mathrm{e}}$. The

output real power P_s from the stator circuit while ignoring the copper loss can be expressed as

$$P_s = -\omega_e T_e = \frac{3}{2}\frac{P}{2}\omega_e \frac{L_m}{L_s}\psi_{ds} i_{qr} \tag{3.30}$$

where ω_e is the synchronous mechanical speed and $\omega_s = \frac{P}{2}\omega_e$ where ω_s is the electric frequency of the stator.

The reactive power from the stator circuit can be expressed as

$$Q_s = -\frac{3}{2}(v_{qs} i_{ds} - v_{ds} i_{qs}) \approx -\frac{3}{2}\frac{P}{2}\omega_e \psi_{ds} i_{ds} \tag{3.31}$$

Note that $\psi_{ds} = L_m i_{dr} + L_s i_{ds}$. When the stator flux is constant, increase (decrease) in i_{dr} results in increase (decrease) in $-i_{ds}$ or Q_s.

Remarks. The output real and reactive power from the stator circuit can be controlled via i_{qr} and i_{dr} respectively. The outer control can be torque/reactive power or torque/AC voltage. In that case, the generator's torque is also only related to i_{qr}.

3.2.2 Inner Current Control

From the outer power control, rotor current references (of the stator flux reference frame) will be generated. It is through the inner current control that the rotor current commands will be followed by the rotor currents. Feedback control will be employed to realize the command tracking.

We will start from the rotor voltage and rotor flux linkage relationship, then derive the rotor voltage and rotor current relationship, and finally find the plant model for current control.

The complex vector model of the rotor voltage/rotor flux linkage is expressed as follows:

$$\overline{V}_r = r_r \bar{I}_r + \frac{d\overline{\psi}_r}{dt} + j\omega_{sl}\overline{\psi}_r \tag{3.32}$$

$$\begin{cases} v_{qr} = r_r i_{qr} + \frac{d\psi_{qr}}{dt} + \omega_{sl}\psi_{dr} \\ v_{dr} = r_r i_{dr} + \frac{d\psi_{dr}}{dt} - \omega_{sl}\psi_{qr} \end{cases} \tag{3.33}$$

Use the condition of stator flux orientation, we have

$$0 = \psi_{qs} = L_{\mathrm{s}} i_{qs} + L_{\mathrm{m}} i_{qr} \tag{3.34}$$

$$\hat{\psi}_{\mathrm{s}} = \psi_{ds} = L_{\mathrm{s}} i_{ds} + L_{\mathrm{m}} i_{dr}. \tag{3.35}$$

Replace the stator currents in the rotor flux linkage expressions by the rotor currents and stator flux linkages:

$$\psi_{qr} = L_{\mathrm{r}} i_{qr} + L_{\mathrm{m}} i_{qs} = \left(L_{\mathrm{r}} - \frac{L_{\mathrm{m}}^2}{L_{\mathrm{s}}} \right) i_{qr} = \sigma L_{\mathrm{r}} i_{qr} \tag{3.36}$$

$$\psi_{dr} = L_{\mathrm{r}} i_{dr} + L_{\mathrm{m}} i_{ds} = L_{\mathrm{r}} i_{dr} + L_{\mathrm{m}} \frac{\psi_{ds} - L_{\mathrm{m}} i_{dr}}{L_{\mathrm{s}}} = \sigma L_{\mathrm{r}} i_{dr} + \frac{L_{\mathrm{m}}}{L_{\mathrm{s}}} \hat{\psi}_{\mathrm{s}} \tag{3.37}$$

The rotor voltages can now be expressed by the rotor currents only:

$$v_{qr} = r_{\mathrm{r}} i_{qr} + \sigma L_{\mathrm{r}} \frac{\mathrm{d}i_{qr}}{\mathrm{d}t} + \omega_{sl} \left(\sigma L_{\mathrm{r}} i_{dr} + \frac{L_{\mathrm{m}}}{L_{\mathrm{s}}} \hat{\psi}_{\mathrm{s}} \right) \tag{3.38}$$

$$v_{dr} = r_{\mathrm{r}} i_{dr} + \sigma L_{\mathrm{r}} \frac{\mathrm{d}i_{dr}}{\mathrm{d}t} - \omega_{sl} \sigma L_{\mathrm{r}} i_{qr} \tag{3.39}$$

Introduce two virtual variables

$$u_{qr} = v_{qr} - \omega_{sl} \left(\sigma L_{\mathrm{r}} i_{dr} + \frac{L_{\mathrm{m}}}{L_{\mathrm{s}}} \hat{\psi}_{\mathrm{s}} \right) \tag{3.40}$$

$$u_{dr} = v_{dr} + \omega_{sl} \sigma L_{\mathrm{r}} i_{qr} \tag{3.41}$$

The plant models can be found as:

$$i_{qr} = \frac{1}{r_{\mathrm{r}} + \sigma L_{\mathrm{r}} s} u_{qr} \tag{3.42}$$

$$i_{dr} = \frac{1}{r_{\mathrm{r}} + \sigma L_{\mathrm{r}} s} u_{dr} \tag{3.43}$$

Feedback controllers can be designed based on the above two first-order plant models to have desired bandwidths. After the feedback controllers, feedforward compensation should be added back to generate the desired rotor voltages.

The overall control diagram is presented in Fig. 3.3. The inner current control design and the output power control design are carried out in two separate steps with the underlying assumption: the dynamics of the current control is much faster than the power control. Separate control design will be carried out for inner current control and outer power control.

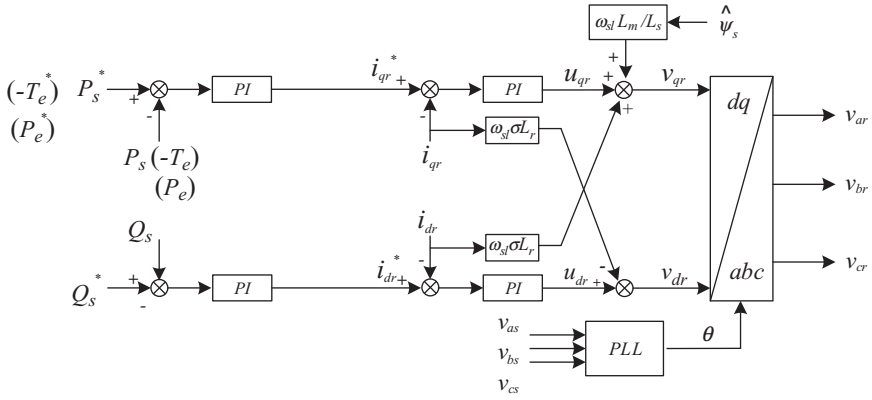

Figure 3.3 DFIG RSC control block diagram.

Indeed, we may be more interested in control of the entire export power or electromagnetic torque from DFIG instead of just the stator power. This can also be done by adjusting i_{qr} only. Recall that

$$P_{\mathrm{s}} = -\omega_{\mathrm{e}} T_{\mathrm{e}} = \frac{3}{2}\frac{P}{2}\omega_{\mathrm{e}}\frac{L_{\mathrm{m}}}{L_{\mathrm{s}}}\psi_{ds} i_{qr}. \tag{3.44}$$

$$P_{\mathrm{e}} = -\omega_{\mathrm{m}} T_{\mathrm{e}} = (1+s)P_{\mathrm{s}} \tag{3.45}$$

If the rotor speed varies much slower than the power control, then we can assume that the slip s is constant and to regulate the entire power P_{e}, we just need to adjust i_{qr}. For a short period of seconds, the wind speed can be assumed as constant. The rotor speed can also be considered as constant.

Additional notes: For the inner current control diagram, the feedforward compensation can be ignored. In that case, to follow a q-axis current command, both qd-axis voltages will be adjusted. Ignoring the feedback compensation makes control simpler and easy to implement. The advantages of feedforward compensation can be found in [4, Chapter 3], including faster start-up transient, decoupling with the AC system, and better disturbance rejection capability.

3.2.3 Maximum Power Point Tracking

Maximum power point tracking (MPPT) can be realized in the RSC control by adjusting the power or torque command. Suppose that the total power

from the DFIG will be controlled. The command of the total power will be generated through the MPPT control block. The input of the control block is the rotor speed ω_m. Through the lookup table, the optimum power corresponding to this speed will be generated. This power will be passed to the outer power control block as the power command.

The ability to get maximum power by the MPPT block is explained as follows. Figure 3.4 presents the wind speed, rotating speed, and mechanical power relationship. The red line (dark grey in print version) is the maximum power curve. Suppose that the wind speed is 9 m/s, the wind generator has a rotating speed lower than the optimum speed. The operating point is notated as Point A, where the optimum operating point is notated as Point B. According to the MPPT lookup table, the generated power command (Point A′) will be less than the current mechanical power. Assuming that the power control dynamics are very fast, the wind turbine now endures a power unbalance: the mechanical power is greater than the electric power. The rotor will speed up until Point B is reached. At Point B, the mechanical power and the electric power command match each other. Similarly, when the wind turbine operates at a rotating speed greater than the optimum speed,

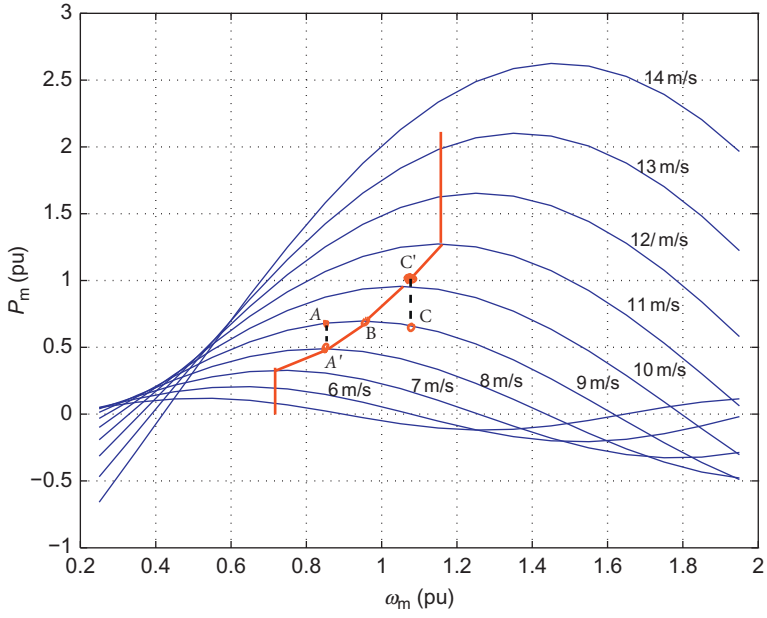

Figure 3.4 MPPT control explanation.

Point C, according to MPPT look up table, the power command should be the same at Point C′. The electric power is now greater than the mechanical power. The rotor should slow down until the operating point reaches B.

3.3 GSC CONTROL

The GSC is connected to the grid through a filter and/or a transformer. The GSC is expected to regulate the AC side voltage/reactive power and to keep the DC-link capacitor voltage constant. With a constant DC-link voltage, the power through the RSC will be the same as that through the GSC. Therefore, this control objective realizes power balance of the converters.

3.3.1 Outer Control

Let the q-axis of the reference frame align with the coupling point voltage $\overrightarrow{e}$ ($e_\mathrm{d} = 0$) and notate the converter output voltage as $\overrightarrow{v}_\mathrm{g}$ or $\overline{V}_\mathrm{g}$. We can then express the real power and reactive power from the GSC to the coupling point as

$$P_\mathrm{g} + jQ_\mathrm{g} = \frac{3}{2}\overline{EI}_\mathrm{g}^{*} \tag{3.46}$$

$$P_\mathrm{g} = \frac{3}{2}(e_q i_{qg} + e_d i_{dg}) = \frac{3}{2} e_q i_{qg} \tag{3.47}$$

$$Q_\mathrm{g} = \frac{3}{2}(e_q i_{dg} - e_d i_{qg}) = \frac{3}{2} e_q i_{dg} \tag{3.48}$$

Therefore, if the coupling point voltage is kept constant (this should be the case for a grid-connected DFIG), real power and reactive power are linearly related to the q-axis and d-axis currents, respectively. We can again design decoupled real power and reactive power control. Keep in mind that the GSC control and RSC control should be coordinated. RSC control has the objective to track the stator active/reactive power commands. Then GSC control should take care of the DC-link voltage.

The DC-link capacitor voltage can be expressed in terms of the power from the RSC and the power leaving the GSC to the grid. The convention of P_r follows the rotor current convention, where injection to the rotor circuit is positive. The convention of P_g follows the GSC current convention, where from the GSC to the grid is positive.

$$\frac{1}{2}C\frac{\mathrm{d}V_\mathrm{dc}^2}{\mathrm{d}t} = -P_\mathrm{r} - P_\mathrm{g} = -\frac{3}{2}\hat{e} i_{qg} - P_\mathrm{r} \tag{3.49}$$

Assuming that the DC-link voltage's variation is small, we have

$$CV_{\mathrm{dc0}}\frac{\mathrm{d}V_{\mathrm{dc}}}{\mathrm{d}t} = -\frac{3}{2}\hat{e}i_{qg} - P_{\mathrm{r}} \tag{3.50}$$

It can be seen that the DC-link voltage can be controlled by adjusting the q-axis current. In this case, positive feedback control should be pursued.

3.3.2 Inner Current Control

The converter is connected to the PCC through an inductor L_{g}. This inductor includes the effect of a filter and/or a transformer. The GSC output voltage, GSC current, and the coupling point voltage have the following relationship expressed in space vector and complex vector.

$$\overrightarrow{v_{\mathrm{g}}} = L\frac{\mathrm{d}\overrightarrow{i}}{\mathrm{d}t} + \overrightarrow{e} \tag{3.51}$$

$$\overline{V}_{\mathrm{g}} = L\frac{\mathrm{d}\bar{I}}{\mathrm{d}t} + \mathrm{j}\omega L_{\mathrm{g}}\bar{I} + \overline{E} \tag{3.52}$$

Align the reference frame's q-axis along with the coupling point voltage $\overrightarrow{e}$, we have

$$v_{qg} = L_{\mathrm{g}}\frac{\mathrm{d}i_{qg}}{\mathrm{d}t} + \omega L_{\mathrm{g}}i_{dg} + e_{\mathrm{q}} \tag{3.53}$$

$$v_{dg} = L_{\mathrm{g}}\frac{\mathrm{d}i_{dg}}{\mathrm{d}t} - \omega L_{\mathrm{g}}i_{qg} \tag{3.54}$$

We can design feedback controllers based on virtual plant inputs $u_{qg} = v_{qg} - \omega L_{\mathrm{g}}i_{dg} - e_{\mathrm{q}}$ and $u_{dg} = v_{dg} + \omega L_{\mathrm{g}}i_{qg}$. The feedback controller has the input from current measurement and generate the desired output u_{qg} and u_{dg}. Through feedforward of cross coupling items, the desired converter voltages can be found.

The overall GSC control is presented in Fig. 3.5. The block LPF stands for a low pass filter which gets rid of high-frequency noise to make the signal smooth. In GSC control, the coupling point voltage is same as the stator voltage.

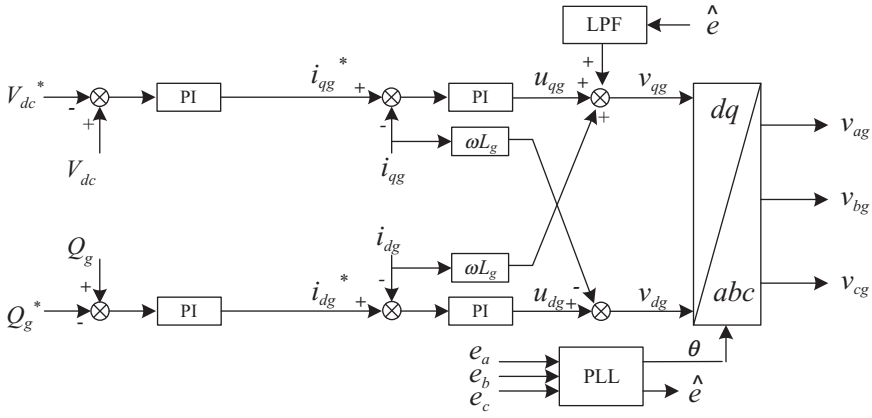

Figure 3.5 DFIG GSC control block diagram.

3.4 COMPLETE DFIG MODELING BLOCKS

RSC and GSC can be considered as two controllable voltage sources. These two voltage sources can be expressed in a reference frame where the stator voltage space vector is aligned with the *q*-axis. Note that the reference frames for DFIG model, RSC control, and GSC control are all aligned with the stator voltage. The RSC and GSC voltages are generated through the afore-mentioned control blocks. In Matlab/Simulink, feedback control blocks can be built. The converter controls can then be integrated with the DFIG model in the same *dq* reference frame.

There is one relationship not modeled yet: the DC-link capacitor dynamics or the relationship between the RSC and the GSC. The DC-link capacitor dynamics has to be considered as well. The overall dynamic model block diagram is shown in Fig. 3.6.

If a DFIG's stator voltage is assumed to be constant, then in the simulation block, v_{qs} can be assumed to be a constant. If the DFIG is connected to an infinity bus through a transmission line which can be considered as series RL components, the transmission line can be regarded as the additional stator resistance and stator leakage inductance. The stator voltage is given from the infinity bus voltage. Should the dynamics of the transmission line are more complicated, then the transmission line has to be adequately modeled. In Chapter 5, dynamics of a transmission line will be modeled and the integrated system model is presented. In Chapter 7, a DFIG

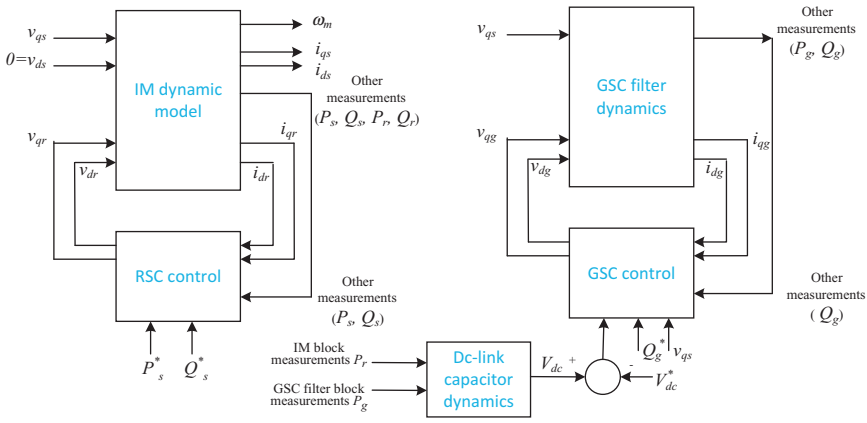

Figure 3.6 Overall DFIG dynamic model block diagram.

is connected to a power grid with multiple synchronous generators. The line dynamics are ignored.

3.5 EXAMPLES

3.5.1 Example 1: PSCAD Simulation of a Two-Level VSC with Sine PWM

In this example, we show PSCAD simulation results of a two-level VSC with sine PWM. The system is shown in Fig. 3.7. The DC side consists of two DC voltage source, each at 100 kV. The DC side is serving an RL three-phase load through a two-level VSC. Six gate signals will be generated through PWM. The phase A voltage (against the ground) v_a, per-phase voltage (E_a, against the neutral point o), and the neutral voltage v_o will be measured.

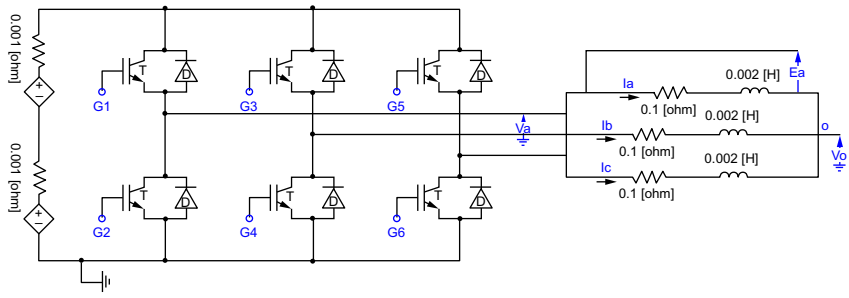

Figure 3.7 A two-level VSC system. DC voltage source: 100 kV.

Figure 3.8 shows the PMW scheme to generate six gate signals. First, three sinusoidal reference signals (magnitude 1, frequency 50 Hz, 120° apart from each other) are generated. The reference signal is then compared with the triangular carrier signal (amplitude 1, frequency 750 Hz). When the reference signal is greater than the carrier signal, the gate signal G1 is 1, G2 is 0. Otherwise, G1 is 0 and G2 is 1. The resulting phase A voltage to the ground is the amplification of the gate signal G1. v_a has two levels: 0 or 200 kV (the DC voltage) as shown in Fig. 3.9. The resulting A to neutral point voltage E_a has five levels as shown in Fig. 3.9. The fundamental component (or the signal after a LPF) is also shown in the first subplot. If we change the frequency and magnitude of the reference signal, we obtain

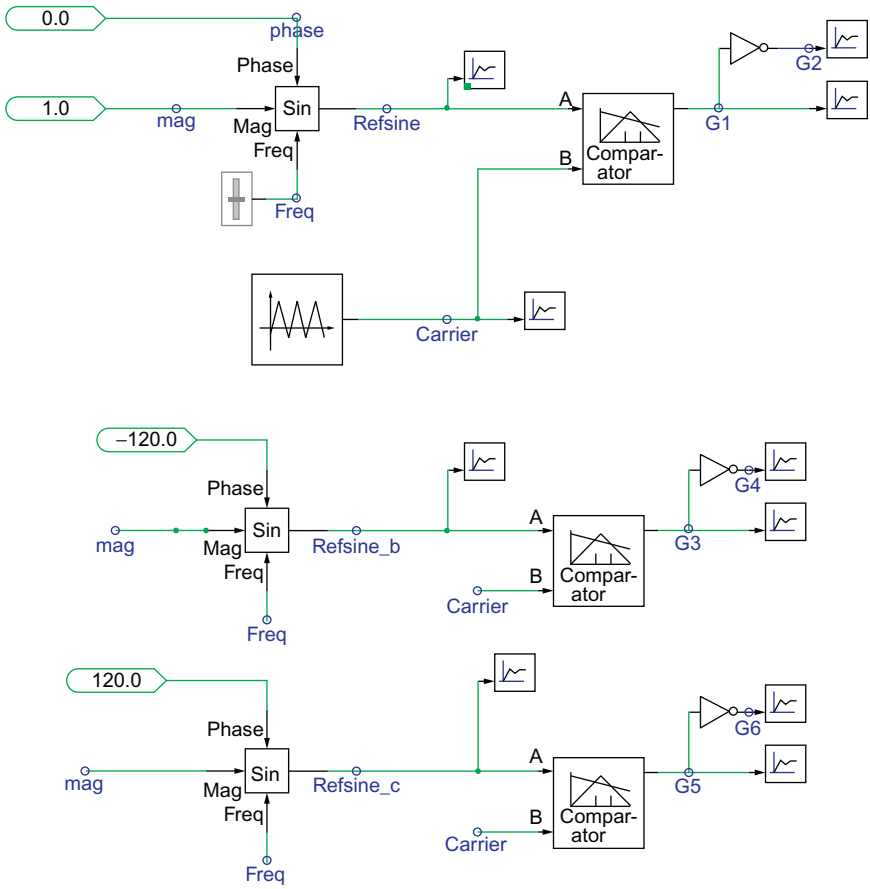

Figure 3.8 Sine PWM schemes for a balanced three-phase output voltage. Modulation index: 1.

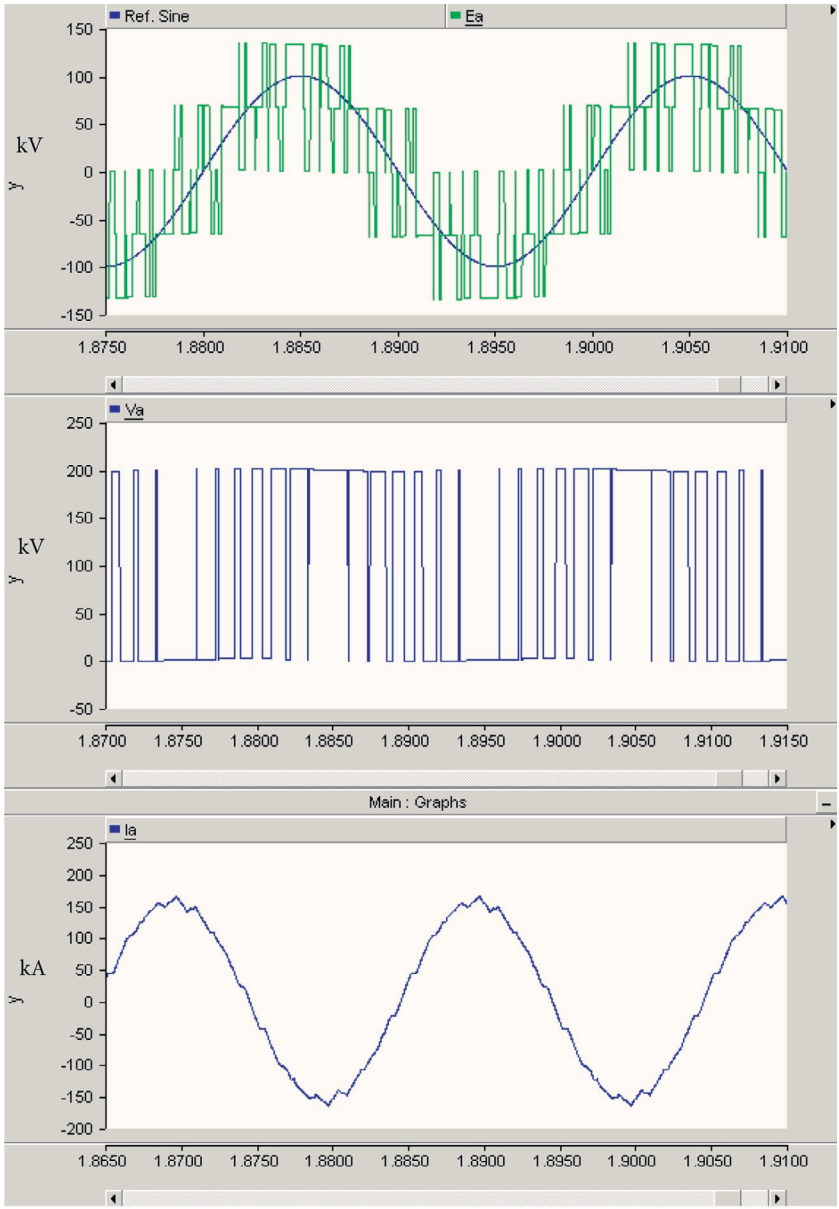

Figure 3.9 Measured signals.

converter voltage with the updated frequency and magnitude. The phase current i_a is shown as almost sinusoidal.

This example gives the PWM switching details and demonstrates that the converter output voltages can be considered as sinusoidal voltages with a fundamental frequency, e.g., 50 Hz. In the mathematical models, the PWM switching details will not be included. Instead, we treat a converter as a controllable three-phase AC voltage source.

3.5.2 Example 2: DFIG Simulation

In the second example, we will use the mathematical model built in Matlab/Simulink to demonstrate DFIG converter control. The dynamic model building follows the diagram shown in Fig. 3.6. The DFIG's parameters are listed in Table 3.1. The slip of the machine is 0.05 pu, which means the DFIG is running below the synchronous speed. Active power will export to the grid through the stator side. However, active power will flow back to the machine rotor ($P_r > 0$, $P_g < 0$) from the grid through GSC and RSC.

Here we assume the stator voltage is constant. At $t = 0.3$ s, the DC-link voltage reference will have a step change. The initial DC voltage reference is 1200 V. After 0.3 s, it becomes 1220 V. We will observe the system dynamic responses in Figs. 3.10–3.12. From Fig. 3.10, it is clear that with GSC control, the DC-link voltage can track the reference. Transients in the DC-link voltage cause transient in the grid converter output active and reactive power.

Table 3.1 Parameters of a Single 2 MW DFIG and the Aggregated DFIG in Network System

Rated power	2 MW
Rated voltage	690 V
X_{ls}	0.09231 pu
X_M	3.95279 pu
X_{lr}	0.09955 pu
R_s	0.00488 pu
R_r'	0.00549 pu
H	3.5 s
X_g	0.3 pu (0.189 mH)
DC-link capacitor C	14,000 μF
DC-link rated voltage	1200 V

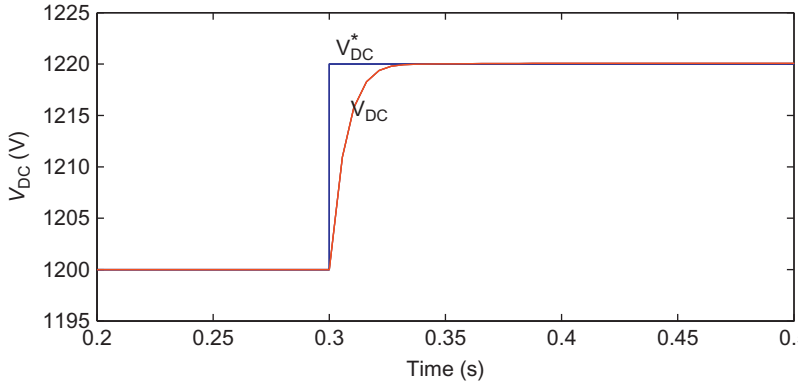

Figure 3.10 DC-Link voltage.

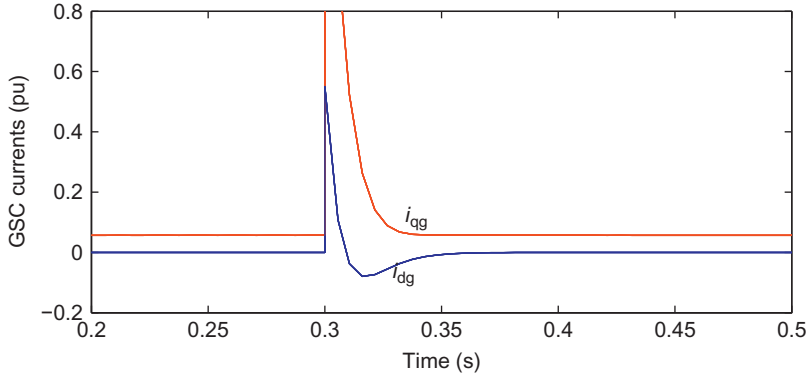

Figure 3.11 GSC qd-axis currents.

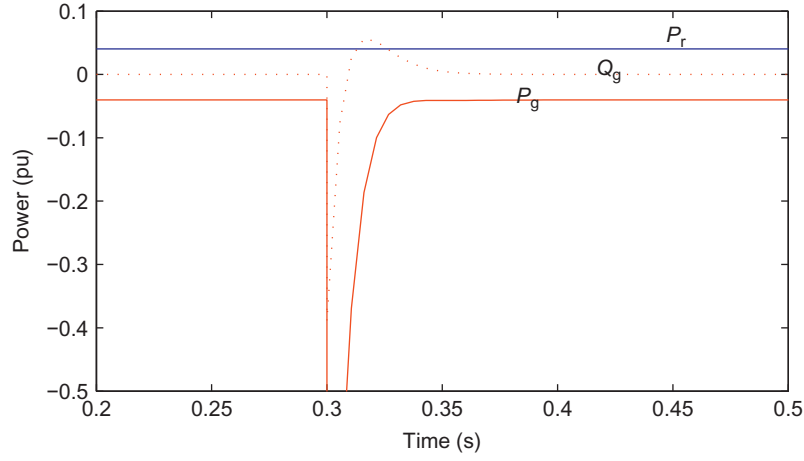

Figure 3.12 Real power from RSC to machine, real and reactive power from GSC to grid.

REFERENCES

[1] B.K. Bose, Modern Power Electronics and AC Drives. Prentice Hall, Upper Saddle River, NJ, 2001.

[2] S.R. Sanders, J.M. Noworolski, X.Z. Liu, G.C. Verghese, Generalized averaging method for power conversion circuits, IEEE Trans. Power Electron. 6(2) (1991) 251-259.

[3] R. Pena, J. Clare, G. Asher, Doubly fed induction generator using back-to-back pwm converters and its application to variable-speed wind-energy generation, IEEE Proc. Electr. Power Appl. 143(3) (1996) 231-241.

[4] A. Yazdani, R. Iravani, Voltage-Sourced Converters in Power Systems: Modeling, Control, and Applications, John Wiley & Sons, New York, 2010.